Power System Stabilizer by using Supplementary Remote Signals

A. A. Hashmani and I. Erlich
Institute of Electrical Power Systems,
University Duisburg-Essen, 47057, Duisburg, Germany
Email: istvan.erlich@uni-due.de

Abstract - This paper presents the design of local H_∞ power system stabilizer (PSS) controller which uses wide-area or global signals as additional measuring information from suitable remote network locations where the oscillations are well observable. The controller, placed at suitably selected generators, provide control signals to the automatic voltage regulators to damp out inter-area oscillations through the machines' excitation systems. Electrical outputs of generators have been used as input signals. To provide robust behavior, H_∞ control theory using an algebraic Riccati equation (ARE) approach has been used to design the proposed controller. The effectiveness of the H_∞ controller is demonstrated through digital simulation studies on a test power system. The simulation results show that the designed controller contributes significantly to the damping of inter-area oscillations and the enhancement of small-signal stability under a wide range of system operating conditions.

Keywords: inter-area oscillations, PSS, remote signals, WAM, robust controller, H_∞ control.

1 INTRODUCTION

As a consequence of deregulation of the electrical energy markets worldwide and the extensions of large interconnected power systems, the tie lines operate near their maximum capacity, especially those connected to the heavy load areas. Stressed operating conditions can increase the possibility of inter-area oscillations between different control areas and even breakup of the whole system [1]. Weakly damped low frequency inter-area oscillations, inherent to large interconnected power systems during transient conditions, are not only dangerous for the reliability and performance of such systems but also for the quality of the supplied energy. With the heavier power transfers ahead, the damping of these oscillations will decrease unless new lines are built (construction of new lines is restricted by environmental and cost factors) or other heavy and expensive high-voltage equipment such as series-compensation is added to the grid's substations. Therefore, achievement of maximum available transfer capability as well as a high level of power quality and security has become a major concern. This concern requires the need for a better coordinated protection and system stability control leading to damping improvement.

It is found that if remote signals from one or more distant locations of the power system are applied to the controller design, the system dynamic performance can be enhanced for a better damping of inter-area oscillations [2]. The remote signals are often referred to as global signals to illustrate the fact that they contain information about overall network dynamics as opposed to local control signals which lack adequate observability of some of the significant inter-area modes [3]. This paper considers a challenging problem which consists in improving the performance of the conventional PSS by using instantaneous measurements from remote locations of the grid.

The recent advances in wide area measurement (WAM) technologies using phasor measurement units (PMUs) can deliver synchronous control signals at high speed [4]. PMUs are deployed at strategic locations on the grid to obtain a coherent picture of the entire network in real time [4]. PMUs measure positive sequence voltage and currents at different locations of the grid. Global positioning system (GPS) technology ensures proper time synchronization among several global signals [4]. The measured global signals are then transmitted via modern telecommunication equipment to the controllers.

Figure 1 describes the basic architecture used in this work. It consists of a set of *n* PSSs located at specially selected generators $G_1,...,G_n$ together with *m* PMUs which are remote to the PSSs. The PSSs are acting on the reference inputs of the voltage regulators. The concept presented in this paper consists of the assumption that the PSS inputs are formed by measured variables coming from the whole system, i.e., particularly also from remote generators [5]. In this way, each PSS receives more complete measuring information about the inter-area oscillations to be damped. It is possible to use any of the variables from the generators, e.g., generator rotor speeds or angles or variables not assigned to generators, e.g. selected tie-line power flows as remote stabilizing signals. In this paper, electrical power outputs of generators, as local and remote measurement feedback signals to the controller, are used to design a two-input, single output controller for a PSS in order to damp out the inter-area oscillations of the study system. In the context of wide-area stabilizing control of bulk power systems, the architecture shown in Figure 1 has higher operational flexibility and reliability, especially when some remote signals are lost. Under such circumstances, the controlled power system is still viable (although with a reduced performance level), owing to the

fact that a fully autonomous and decentralized layer without any communication link is always present to maintain a standard performance level. As the global information is required only for some oscillatory modes, only a few PSS sites with the highest controllability of these modes need be involved in the supplementary global-signal-based actions.

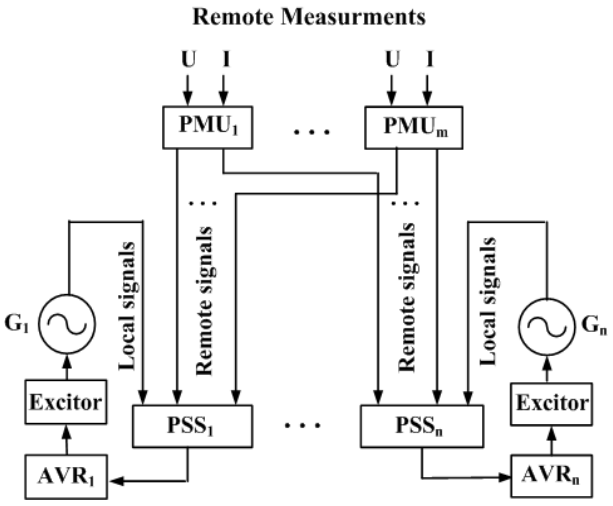

Figure 1: Multimachine power system with PSS using WAMs.

H_∞ based robust control technique is used to design the proposed PSS controller. Digital simulation studies on a two-machine power system are conducted to investigate the effectiveness of the proposed controller during system disturbances. The power system dynamic (PSD) simulation software package [6] is used in this study. PSD allows the simulation of electromechanical oscillations in the time domain and is capable of accomplishing a complete modal analysis of high-dimensional systems using the Arnoldi method [7]. It should be noted that because of the restriction on the number of pages for the paper, the results of modal analysis are not presented in this paper.

The rest of the paper is organized as follows. In Section 2, the design of the proposed H_∞ dynamic output feedback PSS control technique is introduced. In Section 3, a dynamic model of the two-machine system used in this study is discussed. The digital simulation results are presented in Section 4 and the conclusions are discussed in Section 5.

2 ROBUST H_∞ CONTROLLER DESIGN FOR POWER SYSTEMS

2.1 Problem Formulation

The general structure of the *i*th-generator together with the PSS block in a multimachine power system is shown in Figure 2. Inputs of washout filters are electrical power outputs of generators (local and remote) and their outputs are the inputs of the *i*th-controller. The washout filter prevents the controller from acting on the system during steady state.

After augmenting the washout stage in the system, the *i*th-subsystem of the linear, time-invariant, continuous-time composite system which is composed of N subsystems, within the framework of H_∞ design, is described by the following state-space model [8]:

$$\dot{\mathbf{x}}_\mathbf{i}(\mathbf{t}) = \mathbf{A_{ii}}\mathbf{x_i}(\mathbf{t}) + \sum_{\mathbf{j}=1,\mathbf{j}\neq\mathbf{i}}^{\mathbf{N}} \mathbf{A_{ij}}\mathbf{x_j}(\mathbf{t}) + \mathbf{B_{1i}}\mathbf{w_i}(\mathbf{t}) + \mathbf{B_{2i}}\mathbf{u_i}(\mathbf{t}) \quad (1)$$

$$\mathbf{z_i}(\mathbf{t}) = \mathbf{C_{1i}}\mathbf{x_i}(\mathbf{t}) + \mathbf{D_{11i}}\mathbf{w_i}(\mathbf{t}) + \mathbf{D_{12i}}\mathbf{u}(\mathbf{t}) \quad (2)$$

$$\mathbf{y_i}(\mathbf{t}) = \mathbf{C_{2i}}\mathbf{x_i}(\mathbf{t}) + \mathbf{D_{21i}}\mathbf{w_i}(\mathbf{t}) + \mathbf{D_{22i}}\mathbf{u}(\mathbf{t}),\ i=1,\ldots,N \quad (3)$$

where $\mathbf{x_i}(\mathbf{t}) \in \mathbf{R^{n_i}}$ is the state vector, $\mathbf{u_i}(\mathbf{t}) \in \mathbf{R^{m_i}}$ is the control input signals vector, $\mathbf{y_i}(\mathbf{t}) \in \mathbf{R^{p_i}}$ is the measurement output signals vector, $\mathbf{z_i}(\mathbf{t}) \in \mathbf{R^{q_i}}$ is the regulated variables vector including all controlled signals and tracking errors, $\mathbf{w_i}(\mathbf{t}) \in \mathbf{R^{r_i}}$ is the exogenous signals vector including noises, disturbance and reference signals for the *i*th-subsystem and matrices $\mathbf{A_{ii}}$, $\mathbf{A_{ij}}$, $\mathbf{B_{1i}}$, $\mathbf{B_{2i}}$, $\mathbf{C_{1i}}$, $\mathbf{C_{2i}}$, $\mathbf{D_{11i}}$, $\mathbf{D_{12i}}$, $\mathbf{D_{21i}}$ and $\mathbf{D_{22i}}$ are all constant matrices with appropriate dimensions. Moreover, assume that there is no unstable fixed mode [9] with respect to $\begin{bmatrix}\mathbf{C_{21}^T} & \mathbf{C_{22}^T} & \cdots & \mathbf{C_{2N}^T}\end{bmatrix}^\mathbf{T}$, $[\mathbf{A_{ij}}]_{\mathbf{N}\times\mathbf{N}}$ and $\begin{bmatrix}\mathbf{B_{21}^T} & \mathbf{B_{22}^T} & \cdots & \mathbf{B_{2N}^T}\end{bmatrix}^\mathbf{T}$.

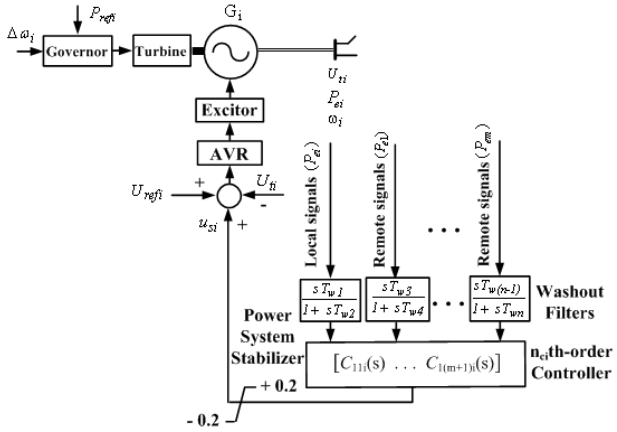

Figure 2: General structure of the *i*th-generator together with the PSS in a multimachine power system.

The complete system can be equivalently described by the following composite equations:

$$\dot{\mathbf{x}}(\mathbf{t}) = \mathbf{A}\mathbf{x}(\mathbf{t}) + \mathbf{B_1}\mathbf{w}(\mathbf{t}) + \mathbf{B_2}\mathbf{u}(\mathbf{t}) \quad (4)$$

$$\mathbf{z}(\mathbf{t}) = \mathbf{C_1}\mathbf{x}(\mathbf{t}) + \mathbf{D_{11}}\mathbf{w}(\mathbf{t}) + \mathbf{D_{12}}\mathbf{u}(\mathbf{t}) \quad (5)$$

$$\mathbf{y}(\mathbf{t}) = \mathbf{C_2}\mathbf{x}(\mathbf{t}) + \mathbf{D_{21}}\mathbf{w}(\mathbf{t}) + \mathbf{D_{22}}\mathbf{u}(\mathbf{t}) \quad (6)$$

where

$$\mathbf{x}(\mathbf{t}) = \begin{bmatrix}\mathbf{x_1^T}(\mathbf{t}) & \mathbf{x_2^T}(\mathbf{t}) & \cdots & \mathbf{x_N^T}(\mathbf{t})\end{bmatrix}^\mathbf{T},$$

$$\mathbf{u}(\mathbf{t}) = \begin{bmatrix}\mathbf{u_1^T}(\mathbf{t}) & \mathbf{u_2^T}(\mathbf{t}) & \cdots & \mathbf{u_N^T}(\mathbf{t})\end{bmatrix}^\mathbf{T},$$

$$\mathbf{y}(\mathbf{t}) = \begin{bmatrix}\mathbf{y_1^T}(\mathbf{t}) & \mathbf{y_2^T}(\mathbf{t}) & \cdots & \mathbf{y_N^T}(\mathbf{t})\end{bmatrix}^\mathbf{T},$$

$$\mathbf{z}(\mathbf{t}) = \begin{bmatrix}\mathbf{z_1^T}(\mathbf{t}) & \mathbf{z_2^T}(\mathbf{t}) & \cdots & \mathbf{z_N^T}(\mathbf{t})\end{bmatrix}^\mathbf{T},$$

$$\mathbf{w}(\mathbf{t}) = \begin{bmatrix}\mathbf{w_1^T}(\mathbf{t}) & \mathbf{w_2^T}(\mathbf{t}) & \cdots & \mathbf{w_N^T}(\mathbf{t})\end{bmatrix}^\mathbf{T} \text{ and}$$

$$\mathbf{A} = [\mathbf{A_{ij}}]_{\mathbf{N}\times\mathbf{N}} = \begin{bmatrix}\mathbf{A_{11}} & \cdots & \mathbf{A_{1N}} \\ \vdots & \ddots & \vdots \\ \mathbf{A_{N1}} & \cdots & \mathbf{A_{NN}}\end{bmatrix},$$

$$\mathbf{B_1} = \mathbf{diag}\{\mathbf{B_{11}}, \mathbf{B_{12}}, \cdots, \mathbf{B_{1N}}\},$$

$$\mathbf{B}_2 = \mathbf{diag}\{\mathbf{B}_{21}, \mathbf{B}_{22}, \cdots, \mathbf{B}_{2N}\},$$
$$\mathbf{C}_1 = \mathbf{diag}\{\mathbf{C}_{11}, \mathbf{C}_{12}, \cdots, \mathbf{C}_{1N}\},$$
$$\mathbf{C}_2 = \mathbf{diag}\{\mathbf{C}_{21}, \mathbf{C}_{22}, \cdots, \mathbf{C}_{2N}\},$$
$$\mathbf{D}_{11} = \mathbf{diag}\{\mathbf{D}_{111}, \mathbf{D}_{112}, \cdots, \mathbf{D}_{11N}\},$$
$$\mathbf{D}_{12} = \mathbf{diag}\{\mathbf{D}_{121}, \mathbf{D}_{122}, \cdots, \mathbf{D}_{12N}\},$$
$$\mathbf{D}_{21} = \mathbf{diag}\{\mathbf{D}_{211}, \mathbf{D}_{212}, \cdots, \mathbf{D}_{21N}\}.$$

The following assumptions are imposed on the plant parameters:

(i) $(\mathbf{A}, \mathbf{B}_2)$ is stabilizable and $(\mathbf{A}, \mathbf{C}_2)$ is detectable;

(ii) $\mathbf{D}_{22} = \mathbf{0}_{p\times m}$;

(iii) $\mathbf{D}_{12}^{\mathrm{T}}[\mathbf{C}_1 \quad \mathbf{D}_{12}] = [0 \quad \mathbf{I}]$ and $\begin{bmatrix}\mathbf{B}_1 \\ \mathbf{D}_{21}\end{bmatrix}\mathbf{D}_{21}^{\mathrm{T}} = \begin{bmatrix}0 \\ \mathbf{I}\end{bmatrix}$.

The dynamic output feedback controller considered for the system of equations (1)-(3) is given by

$$\dot{\mathbf{x}}_{\mathbf{ci}}(\mathbf{t}) = \mathbf{A}_{\mathbf{ci}}\mathbf{x}_{\mathbf{ci}}(\mathbf{t}) + \mathbf{B}_{\mathbf{ci}}\mathbf{y}_{\mathbf{i}}(\mathbf{t}) \tag{7}$$

$$\mathbf{u}_{\mathbf{i}}(\mathbf{t}) = \mathbf{C}_{\mathbf{ci}}\mathbf{x}_{\mathbf{ci}}(\mathbf{t}) + \mathbf{D}_{\mathbf{ci}}\mathbf{y}_{\mathbf{i}}(\mathbf{t}) \tag{8}$$

where $\mathbf{x}_{\mathbf{ci}}(\mathbf{t}) \in \mathbf{R}^{\mathbf{n}_{ci}}$ is the state vector of the ith-local independent controller, n_{ci} is a specified dimension, and $\mathbf{A}_{\mathbf{ci}}$, $\mathbf{B}_{\mathrm{ci}}$, $\mathbf{C}_{\mathbf{ci}}$, $\mathbf{D}_{\mathbf{ci}}$, $i = 1,2,\ldots, N$ are constant matrices to be determined during the design. In this paper, the design procedure deals with $\mathbf{D}_{\mathbf{ci}}$ equal to zero, i.e., $\mathbf{D}_{\mathbf{ci}} = \mathbf{0}$, so that the ith-local independent controller is strictly proper controller.

After augmenting the controller of equations (7) and (8) in the system of equations (1)-(3), the state space equation of the ith-extended subsystem will have the following form:

$$\begin{aligned}\dot{\tilde{\mathbf{x}}}_{\mathbf{i}}(\mathbf{t}) &= (\tilde{\mathbf{A}}_{\mathbf{ii}} + \tilde{\mathbf{B}}_{2\mathbf{i}}\mathbf{K}_{\mathbf{i}}\tilde{\mathbf{C}}_{2\mathbf{i}})\tilde{\mathbf{x}}_{\mathbf{i}}(\mathbf{t}) \\ &\quad + (\tilde{\mathbf{B}}_{1\mathbf{i}} + \tilde{\mathbf{B}}_{2\mathbf{i}}\mathbf{K}_{\mathbf{i}}\tilde{\mathbf{C}}_{2\mathbf{i}})\mathbf{w}_{\mathbf{i}}(\mathbf{t}) + \sum_{\mathbf{j}=1,\mathbf{j}\neq\mathbf{i}}^{\mathbf{N}} \tilde{\mathbf{A}}_{\mathbf{ij}}\tilde{\mathbf{x}}_{\mathbf{j}}(\mathbf{t})\end{aligned} \tag{9}$$

$$\begin{aligned}\mathbf{z}_{\mathbf{i}}(\mathbf{t}) &= (\tilde{\mathbf{C}}_{1\mathbf{i}} + \tilde{\mathbf{D}}_{12\mathbf{i}}\mathbf{K}_{\mathbf{i}}\tilde{\mathbf{C}}_{2\mathbf{i}})\tilde{\mathbf{x}}_{\mathbf{i}}(\mathbf{t}) \\ &\quad + (\tilde{\mathbf{D}}_{1\mathbf{1i}} + \tilde{\mathbf{D}}_{12\mathbf{i}}\mathbf{K}_{\mathbf{i}}\tilde{\mathbf{D}}_{2\mathbf{1i}})\mathbf{w}_{\mathbf{i}}(\mathbf{t})\end{aligned} \tag{10}$$

where $\tilde{\mathbf{x}}_{\mathbf{i}}(\mathbf{t}) = \left[\mathbf{x}_{\mathbf{i}}^{\mathrm{T}}(\mathbf{t}) \quad \mathbf{x}_{\mathbf{ci}}^{\mathrm{T}}(\mathbf{t})\right]^{\mathrm{T}}$ is the augmented state vector for the ith-subsystem and

$$\tilde{\mathbf{A}}_{\mathbf{ij}} = \begin{bmatrix}\mathbf{A}_{\mathbf{ij}} & 0_{\mathbf{n_i}\times\mathbf{n_{ci}}} \\ 0_{\mathbf{n_{ci}}\times\mathbf{n_i}} & 0_{\mathbf{n_{ci}}\times\mathbf{n_{ci}}}\end{bmatrix}, \tilde{\mathbf{B}}_{1\mathbf{i}} = \begin{bmatrix}\mathbf{B}_{1\mathbf{i}} \\ \mathbf{0}_{\mathbf{n_i}\times\mathbf{r_i}}\end{bmatrix}, \tilde{\mathbf{B}}_{2\mathbf{i}} = \begin{bmatrix}\mathbf{0}_{\mathbf{n_i}\times\mathbf{n_{ci}}} & \mathbf{B}_{2\mathbf{i}} \\ \mathbf{I}_{\mathbf{n_{ci}}} & \mathbf{0}_{\mathbf{n_{ci}}\times\mathbf{n_{m_i}}}\end{bmatrix}$$

$$\tilde{\mathbf{C}}_{1\mathbf{i}} = \begin{bmatrix}\mathbf{C}_{1\mathbf{i}} & \mathbf{0}_{\mathbf{p_i}\times\mathbf{n_{ci}}}\end{bmatrix}, \tilde{\mathbf{C}}_{2\mathbf{i}} = \begin{bmatrix}\mathbf{0}_{\mathbf{n_{ci}}\times\mathbf{n_i}} & \mathbf{I}_{\mathbf{n_{ci}}\times\mathbf{n_{ci}}} \\ \mathbf{C}_{2\mathbf{i}} & \mathbf{0}_{\mathbf{q_i}\times\mathbf{n_{ci}}}\end{bmatrix}, \tilde{\mathbf{D}}_{11\mathbf{i}} = \mathbf{D}_{11\mathbf{i}},$$

$$\tilde{\mathbf{D}}_{12\mathbf{i}} = \begin{bmatrix}\mathbf{0}_{\mathbf{p_i}\times\mathbf{n_{ci}}} & \mathbf{D}_{12\mathbf{i}}\end{bmatrix}, \tilde{\mathbf{D}}_{21\mathbf{i}} = \begin{bmatrix}\mathbf{0}_{\mathbf{n_{ci}}\times\mathbf{r_i}} \\ \mathbf{D}_{21\mathbf{i}}\end{bmatrix}, \mathbf{K}_{\mathbf{i}} = \begin{bmatrix}\mathbf{A}_{\mathbf{ci}} & \mathbf{B}_{\mathbf{ci}} \\ \mathbf{C}_{\mathbf{ci}} & \mathbf{D}_{\mathbf{ci}}\end{bmatrix}.$$

Moreover, the overall extended system equation for the system can be rewritten in one state-space equation form as follows:

$$\dot{\tilde{\mathbf{x}}}(\mathbf{t}) = (\tilde{\mathbf{A}} + \tilde{\mathbf{B}}_2\mathbf{K}_{\mathbf{D}}\tilde{\mathbf{C}}_2)\tilde{\mathbf{x}}(\mathbf{t}) + (\tilde{\mathbf{B}}_1 + \tilde{\mathbf{B}}_2\mathbf{K}_{\mathbf{D}}\tilde{\mathbf{C}}_2)\mathbf{w}(\mathbf{t}) \tag{11}$$

$$\mathbf{z}(\mathbf{t}) = (\tilde{\mathbf{C}}_1 + \tilde{\mathbf{D}}_{12}\mathbf{K}_{\mathbf{D}}\tilde{\mathbf{C}}_2)\tilde{\mathbf{x}}(\mathbf{t}) + (\tilde{\mathbf{D}}_{11} + \tilde{\mathbf{D}}_{12}\mathbf{K}_{\mathbf{D}}\tilde{\mathbf{D}}_{21})\mathbf{w}(\mathbf{t}) \tag{12}$$

where

$$\tilde{\mathbf{A}} = \left[\tilde{\mathbf{A}}_{\mathbf{ij}}\right]_{\mathbf{N}\times\mathbf{N}}, \tilde{\mathbf{B}}_1 = \mathbf{diag}\{\tilde{\mathbf{B}}_{11}, \tilde{\mathbf{B}}_{12}, \cdots, \tilde{\mathbf{B}}_{1N}\},$$
$$\tilde{\mathbf{B}}_2 = \mathbf{diag}\{\tilde{\mathbf{B}}_{21}, \tilde{\mathbf{B}}_{22}, \cdots, \tilde{\mathbf{B}}_{2N}\},$$
$$\tilde{\mathbf{C}}_1 = \mathbf{diag}\{\tilde{\mathbf{C}}_{11}, \tilde{\mathbf{C}}_{12}, \cdots, \tilde{\mathbf{C}}_{1N}\},$$
$$\tilde{\mathbf{C}}_2 = \mathbf{diag}\{\tilde{\mathbf{C}}_{21}, \tilde{\mathbf{C}}_{22}, \cdots, \tilde{\mathbf{C}}_{2N}\},$$
$$\tilde{\mathbf{D}}_{11} = \mathbf{diag}\{\tilde{\mathbf{D}}_{111}, \tilde{\mathbf{D}}_{112}, \cdots, \tilde{\mathbf{D}}_{11N}\},$$
$$\tilde{\mathbf{D}}_{12} = \mathbf{diag}\{\tilde{\mathbf{D}}_{121}, \tilde{\mathbf{D}}_{122}, \cdots, \tilde{\mathbf{D}}_{12N}\},$$
$$\tilde{\mathbf{D}}_{21} = \mathbf{diag}\{\tilde{\mathbf{D}}_{211}, \tilde{\mathbf{D}}_{212}, \cdots, \tilde{\mathbf{D}}_{21N}\},$$
$$\tilde{\mathbf{K}}_{\mathbf{D}} = \mathbf{diag}\{\tilde{\mathbf{K}}_1, \tilde{\mathbf{K}}_2, \cdots, \tilde{\mathbf{K}}_{\mathbf{N}}\}.$$

Hence, the overall extended system equation can be rewritten in a compact form as:

$$\dot{\tilde{\mathbf{x}}}(\mathbf{t}) = \mathbf{A}_{\mathbf{cl}}\tilde{\mathbf{x}}(\mathbf{t}) + \mathbf{B}_{\mathbf{cl}}\mathbf{w}(\mathbf{t}) \tag{13}$$

$$\mathbf{z}(\mathbf{t}) = \mathbf{C}_{\mathbf{cl}}\tilde{\mathbf{x}}(\mathbf{t}) + \mathbf{D}_{\mathbf{cl}}\mathbf{w}(\mathbf{t}) \tag{14}$$

where $\mathbf{A}_{\mathbf{cl}} = \tilde{\mathbf{A}} + \tilde{\mathbf{B}}_2\mathbf{K}_{\mathbf{D}}\tilde{\mathbf{C}}_2$, $\mathbf{B}_{\mathbf{cl}} = \tilde{\mathbf{B}}_1 + \tilde{\mathbf{B}}_2\mathbf{K}_{\mathbf{D}}\tilde{\mathbf{C}}_2$,
$\mathbf{C}_{\mathbf{cl}} = \tilde{\mathbf{C}}_1 + \tilde{\mathbf{D}}_{12}\mathbf{K}_{\mathbf{D}}\tilde{\mathbf{C}}_2$, $\mathbf{D}_{\mathbf{cl}} = \tilde{\mathbf{D}}_{11} + \tilde{\mathbf{D}}_{12}\mathbf{K}_{\mathbf{D}}\tilde{\mathbf{D}}_{21}$.

2.2 H_∞ output feedback controller design using Riccati-based approach

Any general system interconnection can be put in the general linear fractional transformation (LFT) framework shown in Figure 3, where **P(s)** is the interconnection matrix, **C(s)** is the controller.

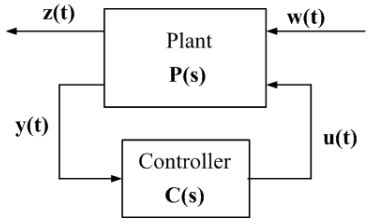

Figure 3: General LFT framework: Feedback interconnection of the plant and the controller systems.

Designing an H_∞ output feedback controller for the system is equivalent to that of finding the matrix $\mathbf{K}_{\mathbf{D}}$ that satisfies an H_∞ norm bound condition on the closed loop transfer function $\mathbf{T}_{\mathbf{zw}}(\mathbf{s}) = \mathbf{C}_{\mathbf{cl}}(\mathbf{sI} - \mathbf{A}_{\mathbf{cl}})^{-1}\mathbf{B}_{\mathbf{cl}}$ from disturbance $\mathbf{w}(t)$ to the controlled variables $\mathbf{z}(t)$ in Figure 3, i.e., $\|\mathbf{T}_{\mathbf{zw}}(\mathbf{s})\|_\infty < \gamma$ (for a given scalar constant $\gamma > 0$). Moreover, transfer functions $\mathbf{T}_{\mathbf{zw}}(\mathbf{s})$ must be stable [10]. An ARE approach [11] can be applied to establish the existence of control strategy of equations (7) and (8) that internally stabilizes the closed loop transfer function $\mathbf{T}_{\mathbf{zw}}(\mathbf{s})$ from disturbance $\mathbf{w}(t)$ to the controlled variables $\mathbf{z}(t)$ and moreover satisfies a certain prescribed disturbance attenuation (or gain) level $\gamma > 0$ on $\mathbf{T}_{\mathbf{zw}}(\mathbf{s})$, i.e., $\|\mathbf{T}_{\mathbf{zw}}(\mathbf{s})\|_\infty < \gamma$. The matrices of dynamic output feedback control law of equations (7) and (8) are given by [11]:

$$\begin{aligned}\mathbf{A}_{\mathbf{ci}} &= \mathbf{A} + (\gamma^{-2}\mathbf{B}_1\mathbf{B}_1^{\mathrm{T}} - \mathbf{B}_2\mathbf{B}_2^{\mathrm{T}})\mathbf{X}_\infty \\ &\quad - (1 - \gamma^{-2}\mathbf{X}_\infty\mathbf{Y}_\infty)^{-1}\mathbf{Y}_\infty\mathbf{C}_2^{\mathrm{T}}\mathbf{C}_2\end{aligned} \tag{15}$$

$$\mathbf{B}_{\mathbf{ci}} = (1 - \gamma^{-2}\mathbf{X}_\infty\mathbf{Y}_\infty)^{-1}\mathbf{Y}_\infty\mathbf{C}_2^{\mathrm{T}} \tag{16}$$

$$\mathbf{C}_{\mathbf{ci}} = -\mathbf{B}_2^{\mathrm{T}}\mathbf{X}_\infty \tag{17}$$

where X_∞ and Y_∞ are the stabilizing solutions of the following AREs:

$$XA + A^T X + X(\gamma^{-2}B_1B_1^T - B_2B_2^T)X + C_1^TC_1 = 0 \tag{18}$$

$$AY + YA^T + Y(\gamma^{-2}C_1^T C_1 - C_2^T C_2)Y + B_1 B_1^T = 0 \quad (19)$$

The output feedback control law of equations (7) and (8) with equations (15)-(17) stabilizes the system of equations (4)-(6) and the closed-loop transfer function matrix $\mathbf{T_{zw}(s)}$ satisfies $\|\mathbf{T_{zw}(s)}\|_\infty < \gamma$.

3 POWER SYSTEM SIMULATION MODEL

The robust dynamic output feedback control design approach presented in the previous section is now applied to a test power system shown in Figure 4. Figure 4 shows a two-machine power system example that has been selected to illustrate the effectiveness of the proposed robust H_∞ controller in damping the system oscillations. The considered system has two identical synchronous generators, each having a rating of 350 MVA and 15.757 kV. Both generators are equipped with identical IEEE standard exciters (IEEE Type DC1A Excitation System). Generator G_2 is equipped with PSS. Load is represented as constant impedance and is connected to bus 5. The fault point *F* is located at bus 3. The generators for these simulations are represented by their fifth-order models. Detailed information about this test system including the controllers and their parameter values can be found in Appendix A. Moreover, for all simulation studies as well as for the PSS design, the structure of the *i*th-generator together with an n_{ci}th-order PSS controller in a multimacine power system, shown in Figure 2, is considered.

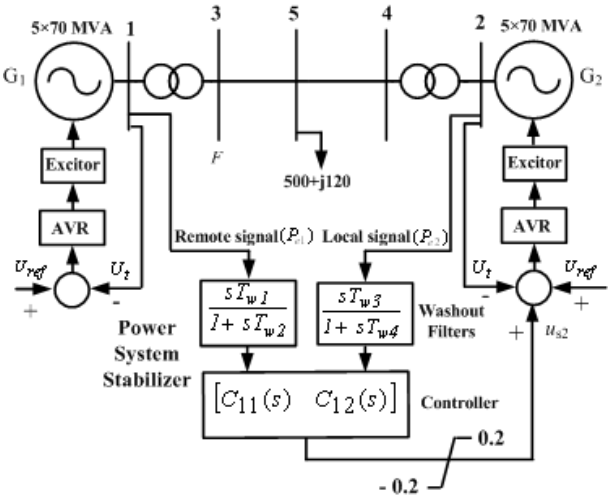

Figure 4: One line diagram of two-machine power system together with the structure of generators and PSS (PSS located at generator G_2).

3.1 Implementation

The base operating conditions are listed in Appendix B. The linearized equations of the two-machine power system of Figure 4 for the given parameter values can be expressed in the general form of equation (4). Therefore, the two-machine power system can be written in the form of system of equations (4)-(6) as:

$$\dot{\mathbf{x}}(\mathbf{t}) = \mathbf{A}\mathbf{x}(\mathbf{t}) + \mathbf{B}_1\mathbf{w}(\mathbf{t}) + \mathbf{B}_2\mathbf{u}(\mathbf{t}) \quad (20)$$

$$\mathbf{z}(\mathbf{t}) = \mathbf{C}_1\mathbf{x}(\mathbf{t}) + \mathbf{D}_{11}\mathbf{w}(\mathbf{t}) + \mathbf{D}_{12}\mathbf{u}(\mathbf{t}) \quad (21)$$

$$\mathbf{y}(\mathbf{t}) = \mathbf{C}_2\mathbf{x}(\mathbf{t}) + \mathbf{D}_{21}\mathbf{w}(\mathbf{t}) \quad (22)$$

where

$\mathbf{x}(\mathbf{t}) = \left[\mathbf{x}_1^{\mathrm{T}}(\mathbf{t}) \quad \mathbf{x}_2^{\mathrm{T}}(\mathbf{t})\right]^{\mathrm{T}}$, $\mathbf{u}(\mathbf{t}) = \left[\mathbf{u}_1^{\mathrm{T}}(\mathbf{t}) \quad \mathbf{u}_2^{\mathrm{T}}(\mathbf{t})\right]^{\mathrm{T}}$,

$\mathbf{y}(\mathbf{t}) = \left[\mathbf{y}_1^{\mathrm{T}}(\mathbf{t}) \quad \mathbf{y}_2^{\mathrm{T}}(\mathbf{t})\right]^{\mathrm{T}}$, $\mathbf{z}(\mathbf{t}) = \left[\mathbf{z}_1^{\mathrm{T}}(\mathbf{t}) \quad \mathbf{z}_2^{\mathrm{T}}(\mathbf{t})\right]^{\mathrm{T}}$,

$\mathbf{w}(\mathbf{t}) = \left[\mathbf{w}_1^{\mathrm{T}}(\mathbf{t}) \quad \mathbf{w}_2^{\mathrm{T}}(\mathbf{t})\right]^{\mathrm{T}}$ and

$\mathbf{A} = \begin{bmatrix} \mathbf{A}_{11} & \mathbf{A}_{12} \\ \mathbf{A}_{21} & \mathbf{A}_{22} \end{bmatrix}$, $\mathbf{B}_1 = \mathbf{diag}\{\mathbf{B}_{11}, \mathbf{B}_{12}\}$,

$\mathbf{B}_2 = \mathbf{diag}\{\mathbf{B}_{21}, \mathbf{B}_{22}\}$, $\mathbf{C}_1 = \mathbf{diag}\{\mathbf{C}_{11}, \mathbf{C}_{12}\}$,

$\mathbf{C}_2 = \mathbf{diag}\{\mathbf{C}_{21}, \mathbf{C}_{22}\}$, $\mathbf{D}_{11} = \mathbf{diag}\{\mathbf{D}_{111}, \mathbf{D}_{112}\}$,

$\mathbf{D}_{12} = \mathbf{diag}\{\mathbf{D}_{121}, \mathbf{D}_{122}\}$, $\mathbf{D}_{21} = \mathbf{diag}\{\mathbf{D}_{211}, \mathbf{D}_{212}\}$.

The state vector $\mathbf{x_1(t)}$ for generator G_1 and AVR of two-machine power system consists of ten state variables. Similarly, state vector $\mathbf{x_2(t)}$ for generator G_2 and AVR consists also of ten state variables. $u_1(t)$ and $u_2(t)$ are control inputs to generators G_1 and G_2 respectively. As in the considered two-machine power system of Figure 4, PSS is located at only generator G_2, therefore, $u_1(t) = 0$ and $u_2(t) = u_{s2}(t)$. In the design, electrical power output signals from both generators are used as measured output feedback signals for robust dynamic output H_∞ based PSS control through the excitation system of generator G_2, i.e., $\mathbf{y(t)} = \left[P_{e1}(t) \quad P_{e2}(t)\right]^T$. Electrical power output of generator G_1 is the remote measured feedback signal to the PSS which is located at the generator G_2 while electrical power output of generator G_2 is the local measured feedback signal to the PSS. Electrical output signals from both generators, the output of the PSS together with the terminal voltage error signals, which are the inputs to the regulator of the exciter, are used as regulated signals within this design framework, i.e., $\mathbf{z(t)} = \left[P_{e1}(t) \quad P_{e2}(t) \quad u_{s2}(t)\right]^T$. The constant matrices for the two-machine power system model of equations (20)-(22) are given in Appendix C.

It is easy to check that $(\mathbf{A}, \mathbf{B_2})$ is stabilizable and $(\mathbf{A}, \mathbf{C_2})$ is detectable. This system is an open loop oscillatory system.

The design procedure of Section 2.2 is used to design a dynamic controller of the form of equations (7) and (8) together with equations (15)-(17) such that minimum disturbance attenuation (from $\mathbf{w(t)} = \left[\mathbf{w}_1^{\mathrm{T}}(\mathbf{t}) \quad \mathbf{w}_2^{\mathrm{T}}(\mathbf{t})\right]^{\mathrm{T}}$ to $\mathbf{z(t)}$) is achieved. Riccati equations (18) and (19) are solved for positive, semi-definitive stabilizing solutions X_∞ and Y_∞ and then H_∞ dynamic output feedback controller is found by using equations (15)-(17) together with equations (7) and (8) by using MATLAB Robust Control Tool box.

3.2 Reduced-Order dynamic output feedback controller Design

The (truncated) balanced realization of the normalized left and right coprime factors of the full order controller has been found and then residualized the balanced realization of the normalized right coprime factors of the full order controller into first-order one using MATLAB. Thus, the H_∞ dynamic output feedback controller obtained is:

$$\left[11.714 \frac{1+s\,0.004}{1+s\,0.0501} \quad 14.999 \frac{1+s\,0.007}{1+s\,0.0501} \right]$$

With this controller, the closed loop system is stable and the H_∞ disturbance attenuation (from **w(t)** to **z(t)**) is $\gamma = 0.0101$.

The performance of the H_∞ control technique will be compared with that of a classical PSS [1] for the two-machine power system shown in Figure 4. The classical PSS is also located at generator G_2. The classical PSS controller has been tuned to a large extent in order to obtain its optimal performance. Bode diagram approach has been used to design the classical PSS controller. The classical controller found is:

$$\left[3.5 \frac{1+s\,0.32}{1+s\,0.069} \quad 10 \frac{1+s\,0.26}{1+s\,0.086} \right]$$

It should be noted that classical PSS used in this study has the same electrical power output signals from both generators, which are used in H_∞ based PSS control, as inputs.

4 SIMULATION RESULTS

The proposed controller in this study is based on the linearized model of the system. However, in order to demonstrate the effectiveness of the proposed controller, extensive simulation studies were conducted. Thus, in the studies, system behavior under large disturbance and wide range of system operating conditions is investigated.

4.1 Large disturbance study

In order to simulate the system behavior under large disturbance conditions, a balanced three-phase fault is applied at bus 3 as shown in Figure 4. The fault sequence of the three-phase fault used in these simulations is as follows:

Fault Sequence:

Stage 1: The system is in pre-fault steady-state.

Stage 2: A fault occurs at $t = 1.0$ s.

Stage 3: The fault is removed and the transmission lines are restored with the fault cleared at $t = 1.1$ s.

Stage 4: The system is in a post-fault state.

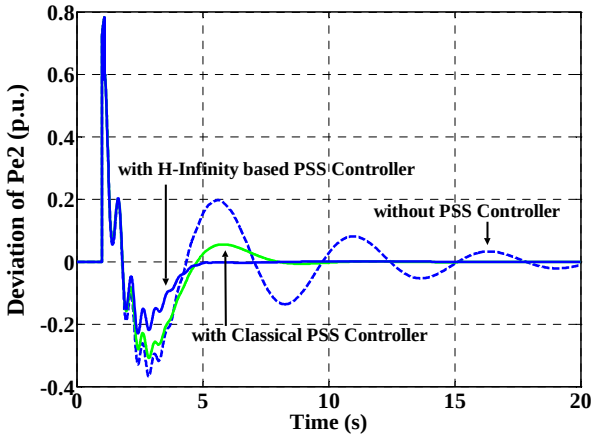

Figure 5: Deviation of P_{e2} following a three-phase fault: Both Local and Remote Signals are available.

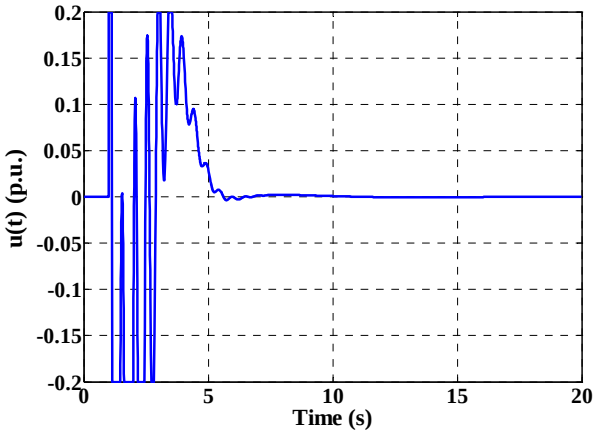

Figure 6: Output of controller following a three-phase fault: Both Local and Remote Signals are available.

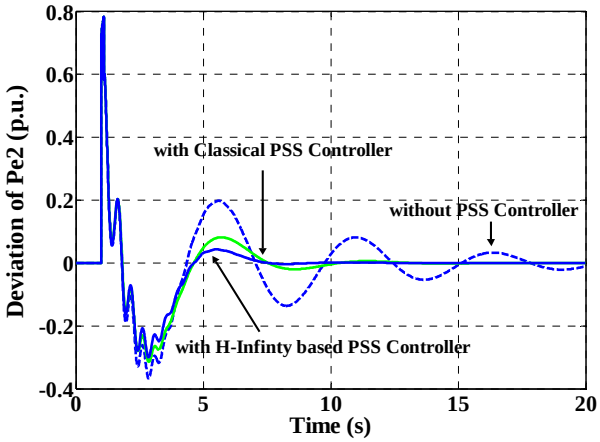

Figure 7: Deviation of P_{e2} following a three-phase fault: Remote Signal is lost.

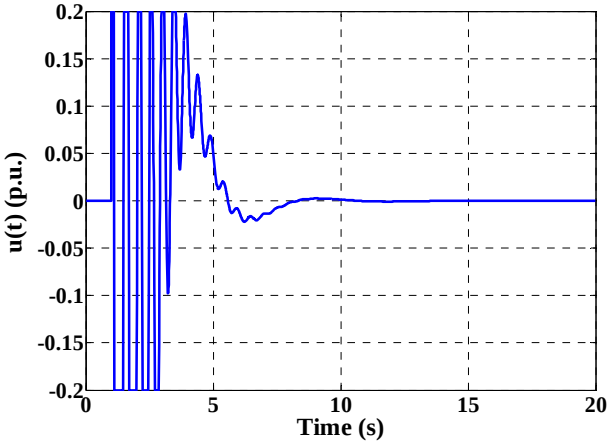

Figure 8: Output of controller following a three-phase fault: Remote Signal is lost.

Simulation results showing the behavior of P_{e2}(t) with and without H_∞ based PSS and classical PSS controls are shown in Figures (5) and (7). Figures (5) and (6) show the behaviors of P_{e2}(t) and u_{s2}(t) when both local and remote signals are used as feedback signals to the PSS while Figures (7) and (8) show the behaviors of P_{e2}(t) and u_{s2}(t) when remote signal is lost. Comparison

of simulation results shown in Figures (5) and (7) indicates that, the system behavior is better when both local and remote signals are used as inputs to the PSS. Figure (7) shows that the system behavior is still effective when remote signal is lost but with the reduced performance level.

4.2 Robustness of proposed controller

To further assess the effectiveness of the proposed approach regarding robustness, the transient performance indices have been computed for different loading conditions at bus 5 [P_L, Q_L]. The transient performance index for electrical power output of the generator following a three-phase short-circuit of 100 ms duration at bus 3 is computed using the following equation:

$$I = \int_0^t \left| P_e(t) - P_{e0}(t) \right| \; dt \qquad (23)$$

For comparison purpose, this index is normalized to the base operating condition for which the controller is designed:

$$I_N = \frac{I_{DLC}}{I_{BLC}} \qquad (24)$$

where I_{DLC} is the transient performance index for different loading condition and I_{BLC} is the transient performance index for base loading condition. The normalized transient performance indices for electrical power output of generator for different loading conditions for proposed H_∞ based PSS controller and classical PSS controller are shown in Figure 9. It can be seen from the figure that the normalized transient performance index for the proposed H_∞ based PSS controller is more near to the unity as compared to the classical PSS controller for wide operating conditions. This clearly indicates that, as compared to the classical PSS controller, the transient response of the generator with the proposed H_∞ based PSS controller for different operating conditions is well damped and the system behavior exhibits robustness for all loading conditions.

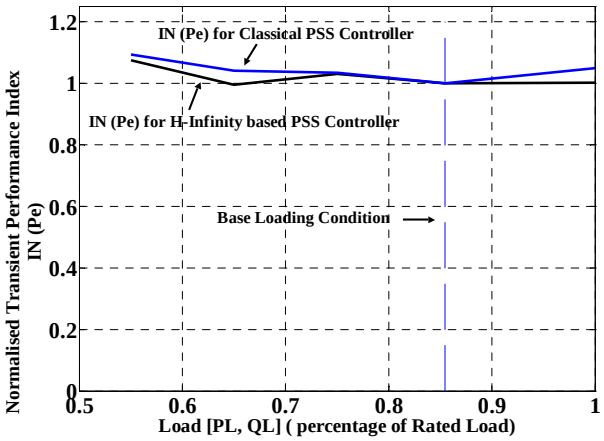

Figure 9: Normalized transient performance index (I_N) for electrical power generated.

Authors are currently investigating the impact of communication delays and the type of remote signals to be used on the performance of the proposed approach. For the selection of remote signals, feature selection techniques [12] are used.

5 CONCLUSIONS

An H_∞ based dynamic output feedback PSS controller using both local and remote signals has been developed. An ARE approach has been used for the design of the full order controller. The full order controller is then reduced to a first order one using model reduction techniques available in MATLAB. The nonlinear simulations results have shown that the proposed controller is effective and robust in suppressing system oscillations for all operating conditions under large disturbances in the system studied. Nonlinear simulation results also show that the proposed controller is effective when the remote signal is lost.

REFERENCES

[1] P. Kundur, "Power System Stability and Control", McGraw-Hill, 1994.

[2] Aaron F. Snyder, Dan Ivanescu, Nouredine HadjSaid, Didier Geroges and Thibault Margotin, "Delay-input Wide-area Stability Control with Synchronized Phasor Measurements", *Proceedings of the* 2000 *IEEE PES Summer Meeting,* vol. 2, pp. 1009-1014.

[3] I. Kamwa R. Grondin. and Y. Hebert, "Wide-area measurement based stabilizing control of large power system-a decentralized/hierarchical approach", *IEEE Transaction on Power Systems,* vol. 16, no. 1**,** pp.136-153, February 2001.

[4] G. Heydt. C. Liu. A. Phadke. and V. Vittal, "Solutions for the crisis in electric power supply", *IEEE Computer Applications in Power***,** pp. 22-30, July 2001.

[5] M. E. Aboul-Ela, A. A. Fouad, J. D. McCalley, A. A. Sallam, "Damping Controller Design for Power System Oscillations using Global Signals", *IEEE Trans. on Power Systems*, vol. 11, pp. 767 - 773, May 1996.

[6] I. Erlich, "Analyse und Simulation des dynamischen Verhaltens von Elektroenergiesystemen", Habilitation-Thesis, Technical University of Dresden, Department of Electrical Engineering, 1995.

[7] R. Lehoucq, K: Machhoff, D. Sorensen, C. Yang, "ARPACK–Arnoldi Package". Available: http://www.caom.rice.edu/software/ARPACK.

[8] G. K. Befekadu and I. Erlich, "Robust Decentralized Controller Design for Power Systems Using Matrix Inequalities Approaches", *IEEE Power Engineering Society General Meeting*, Conference Proceedings, Montreal, QC, Canada, June 18-22, 2006.

[9] S. H. Wang and E. J. Davidson, "On stabilization of decentralized control systems", *IEEE Trans., Autom. Contr.*, vol. 18(5), pp. 473-478, 1973.

[10] P. Gahinet and P. Apkarian, "A linear matrix inequality approach to H_∞ control", *Int. J. Robust & Nonlin. contr*., vol. 4, pp. 421-448, 1994.

[11] John C. Doyle, Keith Glover, Pramod P. Khar gonekar, and Bruce A. Francis, "State-Space Solutions to Standard H_2 and H_∞ Control Problems", *IEEE Transactions on Automatic Control,* vol. 34, No. 8, pp. 831–847, August 1989.

[12] C.A. Jensen, M.A. El-Sharkawi, R.J. Marks II, "Power system security Assessment using Neural networks: Feature selection using Fisher Discrimina tion", *IEEE Transactions on power systems,* vol. 16, No. 4, pp. 757–763, November 2001.

Appendix A

Two-Machine Test System Data

Bus data, line, generator and excitation data are given in this Appendix.

A.1 Synchronous Machines

Parameters: S_r = 70.00 MVA; U_r = 15.75 kV; T_m = 7.00 s; R_a = 0.002 p.u.; X_{sa} = 0.19 p.u.; X_d = 2.49 p.u.; X_q = 2.49 p.u.; $X_d^{'}$ = 0.36 p.u.; $X_d^{''}$ = 0.24 p.u.; $X_q^{'}$ = - ; $X_q^{''}$ = 0.24 p.u.; $T_d^{'}$ = 0.93 s; $T_d^{''}$ = 0.11 s; $T_q^{'}$ = - ; $T_q^{''}$ = 0.2 s.

A.2 Transmission Lines Data

380 kV Line: Single Lines:

$\mathbf{Z}_{11}$ = 0.0309 + j0.266 Ω/km; C_b = 0.0136 μF/km.

A.3 Two Winding Transformers Data

Parameters: r_{ps} [%] = 0.246 ; z_{ps} [%] = 14.203

A.4 Classical automatic voltage regulator (AVR)

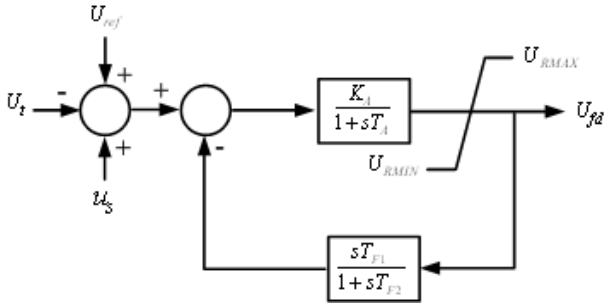

Parameters: K_A = 264 ; T_A = 0.33 s; T_{F1} = 0.2 s; T_{F2} = 1.0 s; U_{RMAX} = 7.0 p.u.; U_{RMIN} = -7.0 p.u.

A.5 Power system stabilizer (PSS)

Parameters: T_{w1} = 0.05 s; T_{w2} = 0.1 s; T_{w3} = 0.05 s; T_{w4} = 0.01 s.

Appendix B

The system is operating with generating units loaded as follows:

G_1:P=250 MW;Q=7.57 MVAr; $\mathbf{U}_t$=15.75 kV$\angle$ - 23.06° .

G_2:P=252.58MW;Q=2.83MVAr;$\mathbf{U}_t$=15.75kV$\angle$ - 23.12°

The load at bus 5: P_L = 500 MW, Q_L = 120 MVAr.

Appendix C

Constant matrices for the two-machine power system model of equations (20)-(22) are as follows:

$$\mathbf{A}_{11}=\begin{bmatrix}
-1.5988 & 0.5082 & 0.012 & 0 & -0.038 & 0 & 0 & 0 & 0.0376 & 0\\
75.6076 & -39.09 & 1.7909 & 0 & -5.6573 & 0 & 0 & 0 & 0 & 0\\
-0.9557 & -0.9557 & -4.494 & 0 & -1.2694 & 0 & 0 & 0 & 0 & 0\\
-0.2754 & -0.2754 & 0.0178 & 0 & -0.2111 & 0 & 0 & 0 & 0 & 0\\
0 & 0 & 0 & 314.1593 & 0 & 0 & 0 & 0 & 0 & 0\\
-192.7667 & -192.7667 & 12.4907 & 0 & -147.7462 & -100 & 0 & 0 & 0 & 0\\
-14.4327 & -14.4327 & 19.6464 & 0 & 0.9096 & 0 & -40 & 0 & 0 & 0\\
0 & 0 & 0 & 0 & 0 & 0 & 800 & -163.0303 & 0 & 800\\
0 & 0 & 0 & 0 & 0 & 0 & 0 & 2.0408 & -2.0408 & 0\\
0 & 0 & 0 & 0 & 0 & 0 & 0 & 0.2 & 0 & -1
\end{bmatrix}$$

$$\mathbf{A}_{12}=\begin{bmatrix}
0.0372 & 0.0372 & 0.0122 & 0 & 0.038 & 0 & 0 & 0 & 0 & 0\\
5.5355 & 5.5355 & 1.8081 & 0 & 5.6573 & 0 & 0 & 0 & 0 & 0\\
-0.9665 & -0.9665 & 2.9542 & 0 & 1.2694 & 0 & 0 & 0 & 0 & 0\\
0.1149 & 0.1149 & 0.1733 & 0 & 0.2111 & 0 & 0 & 0 & 0 & 0\\
0 & 0 & 0 & 0 & 0 & 0 & 0 & 0 & 0 & 0\\
80.3986 & 80.3986 & 121.3129 & 0 & 147.7462 & 0 & 0 & 0 & 0 & 0\\
-9.5097 & -9.5097 & 9.6623 & 0 & -0.9096 & 0 & 0 & 0 & 0 & 0\\
0 & 0 & 0 & 0 & 0 & 0 & 0 & 0 & 0 & 0\\
0 & 0 & 0 & 0 & 0 & 0 & 0 & 0 & 0 & 0\\
0 & 0 & 0 & 0 & 0 & 0 & 0 & 0 & 0 & 0
\end{bmatrix}$$

$$\mathbf{B}_1=\begin{bmatrix}0 & 0 & 0 & 0 & 0 & 0 & 0 & 0 & 0 & 0\end{bmatrix}^{\mathbf{T}}$$

$$\mathbf{A}_{21}=\begin{bmatrix}
0.0276 & 0.0276 & 0.0058 & 0 & 0.026 & 0 & 0 & 0 & 0 & 0\\
1.1806 & 1.1806 & 0.2498 & 0 & 1.1136 & 0 & 0 & 0 & 0 & 0\\
-0.317 & -0.317 & 1.4981 & 0 & 0.7024 & 0 & 0 & 0 & 0 & 0\\
0.1284 & 0.1284 & 0.1694 & 0 & 0.2122 & 0 & 0 & 0 & 0 & 0\\
0 & 0 & 0 & 0 & 0 & 0 & 0 & 0 & 0 & 0\\
81.7225 & 81.7225 & 107.8278 & 0 & 135.0132 & 0 & 0 & 0 & 0 & 0\\
-8.9695 & -8.9695 & 10.1657 & 0 & -0.7424 & 0 & 0 & 0 & 0 & 0\\
0 & 0 & 0 & 0 & 0 & 0 & 0 & 0 & 0 & 0\\
0 & 0 & 0 & 0 & 0 & 0 & 0 & 0 & 0 & 0\\
0 & 0 & 0 & 0 & 0 & 0 & 0 & 0 & 0 & 0
\end{bmatrix}$$

$$\mathbf{A}_{22}=\begin{bmatrix}
-1.5983 & 0.3677 & 0.0089 & 0 & -0.026 & 0 & 0 & 0 & 0.0427 & 0\\
15.7402 & -6.3054 & 0.3826 & 0 & -1.1136 & 0 & 0 & 0 & 0 & 0\\
-0.4855 & -0.4855 & -2.1943 & 0 & -0.7024 & 0 & 0 & 0 & 0 & 0\\
-0.2744 & -0.2744 & 0.0094 & 0 & -0.2122 & 0 & 0 & 0 & 0 & 0\\
0 & 0 & 0 & 314.1593 & 0 & 0 & 0 & 0 & 0 & 0\\
-174.642 & -174.642 & 5.965 & 0 & -135.0132 & -90.9091 & 0 & 0 & 0 & 0\\
-15.9639 & -15.9639 & 19.5096 & 0 & 0.7424 & 0 & -40 & 0 & 0 & 0\\
0 & 0 & 0 & 0 & 0 & 0 & 800 & -163.0303 & 0 & 800\\
0 & 0 & 0 & 0 & 0 & 0 & 0 & 2.0408 & -2.0408 & 0\\
0 & 0 & 0 & 0 & 0 & 0 & 0 & 0.2 & 0 & -1
\end{bmatrix}$$

$$\mathbf{B}_2=\begin{bmatrix}0 & 0 & 0 & 0 & 0 & 0 & \dfrac{1}{0.025} & 0 & 0 & 0\end{bmatrix}^{\mathbf{T}}$$

Let

$$\mathbf{C}_{11}=\begin{bmatrix}0 & 0 & 0 & 0 & 0 & 1 & 0 & 0 & 0 & 0\end{bmatrix}$$

$$\mathbf{C}_{12}=\begin{bmatrix}0 & 0 & 0 & 0 & 0 & 1 & 0 & 0 & 0 & 0\\ 0 & 0 & 0 & 0 & 0 & 0 & 0 & 0 & 0 & 0\end{bmatrix}$$

$$\mathbf{C}_{21}=\mathbf{C}_{22}=\begin{bmatrix}0 & 0 & 0 & 0 & 0 & 1 & 0 & 0 & 0 & 0\end{bmatrix}$$

$$\mathbf{D}_{111}=\begin{bmatrix}0\end{bmatrix},\mathbf{D}_{112}=\begin{bmatrix}0 & 0\end{bmatrix}^{\mathbf{T}},\mathbf{D}_{121}=\begin{bmatrix}0\end{bmatrix},$$

$$\mathbf{D}_{122}=\begin{bmatrix}0 & 0.001\end{bmatrix}^{\mathbf{T}},\mathbf{D}_{211}=\mathbf{D}_{212}=\begin{bmatrix}0\end{bmatrix}.$$